Preprints.org

Article

Not peer-reviewed version

Experimental Study of Two-Bite Test Parameters for Effective Drug Release from Chewing Gum Using a Novel Bio-Engineered Testbed

Kazem Alemzadeh * and Joseph Alemzadeh

Posted Date: 16 June 2025

doi: 10.20944/preprints202506.1212.v1

Keywords: Humanoid Chewing Robot; Biomimetic Chewing Chamber; Occluded Molars; Chewing Efficiency; Effective Mastication; Crush/Shear Ratio; Bionics; Dental Morphology and Jaws physiology; FMA and BA angles; Two-bite Test; Medicated Chewing Gum; Mechanochemistry; Work Done

Preprints.org is a free multidisciplinary platform providing preprint service that is dedicated to making early versions of research outputs permanently available and citable. Preprints posted at Preprints.org appear in Web of Science, Crossref, Google Scholar, Scilit, Europe PMC.

Copyright: This open access article is published under a Creative Commons CC BY 4.0 license, which permit the free download, distribution, and reuse, provided that the author and preprint are cited in any reuse.

Preprints.org (www.preprints.org) | NOT PEER-REVIEWED | Posted: 16 June 2025 doi:10.20944/preprints202506.1212.v1

Disclaimer/Publisher's Note: The statements, opinions, and data contained in all publications are solely those of the individual author(s) and contributor(s) and not of MDPI and/or the editor(s). MDPI and/or the editor(s) disclaim responsibility for any injury to people or property resulting from any ideas, methods, instructions, or products referred to in the content.

Article

Experimental Study of Two-Bite Test Parameters for Effective Drug Release from Chewing Gum Using a Novel Bio-Engineered Testbed

Kazem Alemzadeh [1,*] and Joseph Alemzadeh [2]

[1] Faculty of Engineering, School of Electrical, Electronic and Mechanical Engineering, (ESDI) Bionics and Bioengineering Research Group, University of Bristol, Bristol BS8 1TR, UK

[2] Alumnus of the Cardiff University

* Correspondence: k.alemzadeh@bristol.ac.uk

Abstract: Background: A critical review of the literature demonstrates that masticatory apparatus with an artificial oral environment is of interest in fields including i) dental science; ii) food science; and iii) the pharmaceutical industries for drug release. However, apparatus that closely mimics human chewing and oral conditions has yet to be realised. This study investigates the vital role of dental morphology and form-function connections using two-bite test parameters for effective drug release from medicated chewing gum (MCG) and compares them to human chewing efficiency with the aid of a humanoid chewing robot and a bionics product lifecycle management (PLM) framework with built-in reverse biomimetics – both developed by the first author. **Methods**: A novel, bio-engineered two-bite testbed is created for two testing machines with compression and torsion capabilities to conduct two-bite tests for evaluating the mechanical properties of MCGs. **Results**: Experimental studies are conducted to investigate the relationship between biting force and crushing/shearing and understand chewing efficiency and effective mastication. This is with respect to mechanochemistry and power stroke for disrupting mechanical bonds releasing active pharmaceutical ingredients (APIs) of MCGs. The manuscript discusses the effect and the critical role that jaw physiology, dental morphology, Bennett angle of mandible (BA) and the Frankfort-mandibular plane angle (FMA) on two-bite test parameters when FMA = 0, 25 or 29.1 and BA = 0 or 8. **Conclusions:** Impact for other scientific fields is also explored.

Keywords: humanoid chewing robot; biomimetic chewing chamber; occluded molars; chewing efficiency; effective mastication; crush/shear ratio; bionics; dental morphology and jaws physiology; FMA and BA angles; two-bite test; medicated chewing gum; mechanochemistry; work done

1. Introduction

Over the last four decades masticatory apparatus has rapidly developed. A review of the literature demonstrates that apparatus with an artificial oral environment is of interest to fields including i) dental science where the focus is on material testing and failure points [1–3]; ii) food science that focuses on bolus breakdown for flavour release [4–7], and iii) the pharmaceutical industry for drug release [8,9]. However, instruments that closely mimic human chewing and oral conditions have yet to be realised [10].

Regardless of applications, during the design process of bio-inspired products there is a trade-off [11] when seeking alternative designs for optimum solutions. Trade-offs are inherent features of many biomechanical systems and are often seen as evolutionary constraints. Structural decoupling and abstraction of the relationship may provide a way to overcome those limits in some systems but not for the form-function structures that transmit large forces, such as mammalian mandibles [12]. A brief, yet critical, review these trade-offs are listed below, for *in vitro* apparatus within dental/food science and pharmaceutical industry.

© 2025 by the author(s). Distributed under a Creative Commons CC BY license.

Preprints.org (www.preprints.org) | NOT PEER-REVIEWED | Posted: 16 June 2025 doi:10.20944/preprints202506.1212.v1

Within dental science on wear and microwear, a study by Heintze and co-workers study [13] concluded that: i) mimicking the entire masticatory cycle with all possible movements of the lower jaw is not necessarily the best approach, and ii) a machine that applies a force in only one direction is also inadequate. Krueger and co-workers [14] highlighted the uncertainties surrounding the mechanisms underlying its formation due to a lack of standardisation across *in vitro* studies. Daegling and co-workers [15] mentioned that utilising various chewing simulators or mechanical testing systems may help. However, these studies are utilising different chewing simulators, methodologies for tooth preparation, and species used in analysis which inhibits effective comparisons across studies.

Within food science on aroma release, the recent review by Pu and co-workers [16] summarised the latest developments in aroma release from food to the retronasal cavity, aroma release and delivery influencing factors, and aroma perception mechanisms. They identified that it is necessary to develop more accurate *in vitro* equipment for simulating the procedures during oral processing. Their study looked at four chewing simulators developed by [6,10,17,18] for food oral processing and they suggested that intelligent chewing simulators are is key to establish a standard analytical method.

On physiological structures of masticatory simulators and oral cavity, Guo and co-workers [19] comprehensive review of systematic designs from the past 15 years highlighted the current limitations of these simulators and stated there is no established standard method and criteria for evaluating their biomimetic components. Their work suggested that it is essential to introduce innovative equipment and testing methods for standardising chewing efficiency, plus criteria for evaluating the biomimetic components of those simulators.

On the effect of dental morphology, form-function and comminution, Walker and co-workers [20] investigated the effect of these factors with attention to comminution chewing experiments in catarrhines. Molars intercuspation was used as tools to perform different food processing actions such as crushing and shearing. Their study reviewed the state of the art, chewing experiments and investigated the effects of molar morphology on chewing efficiency with one pair of opposite upper and lower second molars. The chewing simulator used in their study was developed by Salles and co-workers [6] for food fracturing which is equipped with two dental replica rings having equal size teeth as human jaws. Simplification of humans jaws (i.e. as a trade-off) was apparent, although tooth size has an influence on the fragmentation of certain types of food, in terms of mechanics [21–23]. They concluded that due to limitations of the chewing simulator, the design of a new chewing simulator is underway that will improve the emulation of natural masticatory processes is underway. Other simulators under development [10,14,24,25] may allow further studies on form-function relationships of teeth.

Within the pharmaceutical industry, drug release from a medicated chewing gum (MCG) is an advanced drug delivery method with a promising future [26,27]. A major advantage of delivering pharmaceutical drugs through chewing gum, rather than conventional tablets, lies in the absorption of the drug through the oral mucosa. This avoids metabolism in the gastrointestinal tract and reducing first pass metabolism. Because of absorption through the oral mucosa, it is possible that a lower concentration of the drug can be prescribed due to greater bioavailability and faster onset of action if delivered this way [28,29]. In addition to health benefits, the potential reduction in the active pharmaceutical ingredient (API) can both reduce cost and increase availability and accessibility of MCGs across the globe. For example, MCGs containing casein phosphopeptide-amorphous calcium phosphate (CPP-ACP) were shown to protect against tooth decay [30,31] which was reported to affect 2.4 billion people worldwide in 2010 [32] and more than 35% globally in 2020 [33]. Other MCG examples contain aspirin, caffeine, dimenhydrinate, vitamin C and chlorhexidine [28]. The global markets for aspirin and vitamin C are $3bn and $1.8bn respectively [34,35], meaning a reduction in API of 10%-20% could result in savings of $0.5bn per annum. Recent studies suggest curcumin (CUR) chewing gums have potential therapeutic benefits to head and neck cancer patients [28,36,37], and

© 2025 by the author(s). Distributed under a Creative Commons CC BY license.

Preprints.org (www.preprints.org) | NOT PEER-REVIEWED | Posted: 16 June 2025 doi:10.20944/preprints202506.1212.v1

angiotensin-converting enzyme-2 chewing gums have been shown to decrease oral virus transmission and infection of SARS-CoV-2 [38].

The potential and the health benefits of MCGs [39] have not yet been fully exploited [40] due to:

1) the inherent technical and scientific challenges in realising *in vitro* apparatus to test drug release prior to human studies. These challenges arise from the need to replicate the intricate jaws physiology and human oral environment with masticatory motions and forces, and the flow of saliva over the artificial gum surface necessary for the release of the API from the MCG [10].

2) complexity of their formulation, lack of acceptable testing methods, and intricacy of their manufacturing. Due to the scarcity of studies concerning the evaluation of the mechanical properties of MCGs [28,37,41,42]

The current state of the art described in the European Pharmacopeia [43] includes Apparatus A [8] and B [9] developed by Christrup and Møller 1986 and Kvist et al., 1999 respectively for *in vitro* drug release testing [28]. However, they yield inconsistent results and fail to accurately simulate the complex chewing motions and forces. Moreover, they cannot combine mastication, saliva, and chewing gum together to mimic human oral conditions to allow the measurement of the release of APIs effectively from MCG and thus are not widely accepted or FDA-approved for this reason [10,44–47].

A review of methods A & B by Stomberg and co-workers [44] in 2017 indicated that they simplify mastication to a stamping procedure between two flat-faced, optionally rotating pistons. They developed a 45º gliding steel unit with a four-cylindrical-cusped molar [44], which attempted to imitate the occlusal plane of the natural dentition with the simulator squeezing the gum by a pre-set deformation force [44]. However, despite the authors' valiant attempts, the four cusped molar tooth apparatus had limited anatomical accuracy, and the occlusal surface geometries and mastication was very simplified [44].

A more recent review of A & B apparatus by Externbrink and co-workers [46] highlighted a need for new testing methodologies to evaluate the performance of potentially abuse-deterrent opioid products by chewing. They mentioned that Apparatus B has been described in the scientific literature and is commercially available (Erweka release tester, Erweka GmbH). They used Apparatus B and their study indicates that the chewing methodology evaluated in their work may provide a useful *in vitro* tool to characterise chewing resistance and API release properties. However, Apparatus B provides a simplified and standardised model of the human jaw with limited capability to fully mimic the complex physiological conditions in the oral cavity during chewing.

Alemzadeh and co-workers created a novel chewing robot with built-in humanoid jaws as an artificial oral environment with temperature-control and artificial saliva, capable of closely replicating the human chewing motion. This allowed for the measurement of xylitol release from commercially available chewing gum which was quantified following both *in vitro* and *in vivo* mastication. The chewing robot demonstrated a similar release rate of xylitol as human participants [10].

Currently, there is no information that exists on the morphology of occluded pairs of maxillary and mandibular molars in any of the bio-inspired chewing simulators. Specifically, no biomimetic standard design processes with their associated tools could be found on how accurately these were abstracted from a biological pair and biomimetically modelled and realised, as highlighted by Guo and co-workers in their comprehensive review in 2024 [19].

In this respect, Alemzadeh [48] proposed a bionics product-life cycle management (PLM) methodology with built-in reverse biomimetics for innovative product development. The novel PLM framework utilising bionics aimed at aiding knowledge transfer from biology to engineering to maintain the accuracy and integrity of form-function relationships during the processes of identification and knowledge transfer between anatomical landmarks and biological structures. The proposed framework supported by technical biology as an enabling method for abstracting the geometrical biological structures to obtain design intents, removes the limitations of the biomimetic processes facing engineering. The study systematically illustrated knowledge transfer methodology

© 2025 by the author(s). Distributed under a Creative Commons CC BY license.

Preprints.org (www.preprints.org) | NOT PEER-REVIEWED | Posted: 16 June 2025 doi:10.20944/preprints202506.1212.v1

in a step-by-step manner to analyse and reveal the constructional design and working principles of large-scale, human skeletal biological systems in nature. Alemzadeh's study [48] presented comprehensive processes of bionic design and biomimetic modelling, simulation, optimisation, and validation techniques necessary for a drug-releasing chewing robot and an anthropometric prosthetic hand.

This investigation herein explores the vital role of jaws physiology, dental morphology and form-function on two-bite tests, also known as texture profile analysis (TPA). While TPA is a standard method for determining the textural or mechanical properties in food science [49], it is an unofficial product quality tests in pharmaceutical industry for drug release of solid/semi-solid oral dosage forms, such as tablets, chewable tablets, MCGS, and others [28,36,37,41,50,51]. In the latest review by Bogdan and co-workers [51] in 2023 texture analysis was identified as a versatile tool but challenging, due to different experimental conditions, the choice of testing protocol and parameters. Their study provided guidelines for the use of universal testing system and texture analysers with their parameters set ups for pharmaceutical products such as tablets and chewable tablets.

In this study a novel, bio-engineered two-bite testbed with compression and torsion capabilities was created for two universal testing machines to investigate TPA parameters for evaluating the mechanical properties of MCGs [28,37,41]. Moreover, it compares this to human chewing efficiency with the aid of a humanoid chewing robot and a bionic-related PLM framework with built-in reverse biomimetics – both developed by Alemzadeh [10,48]. The testbed integrates an occluded pair of maxillary and mandibular molars used in the humanoid chewing chamber [10], and the bionics PLM framework [48] is incorporated to address current issues surrounding the instrumentation to conduct two-bite tests [52] and inconsistencies that currently exist with *in vitro* masticatory apparatus as analysed in Section 1.

Experimental studies were conducted to systematically analyse a bio-inspired mastication and to probe the form-function relationships between biting force and crushing/shearing aspects for understanding chewing efficiency in relation to mechanochemistry and power stroke for disrupting mechanical bonds. Discussion is given on the effect that different molar morphologies, the Frankfort-mandibular plane angle (FMA) and Bennett angle (BA) have on TPA parameters. Finally, impact for other scientific fields is also explored.

2. Materials and Methods

The Novel Two-bite Bio-engineered Testbed

2.1. Design and Modelling of Maxillary-Mandibular-Bio Testbed

The novel testbed is based on design methodology principles from bionics proposed by Alemzadeh [48], allowing for accurate comminution and molars intercuspation to investigate the mechanics of chewing sequences, crushing, shearing, and grinding. The testbed uses the exact copy of an occluded pair of maxillary and mandibular molars which are built into the artificial oral environment that has been validated with human participants [10] prior to this investigation as shown in Figure 1. The universal testing machines used were the 50KN 2580 Static Load Cell (Instron, UK) and Amslet HCT 25 (Zwick-Roell, UK). The latter is capable of human chewing frequency (a 49.5 mm/s compression speed), whilst the former is not, so 10 mm/s was also tested.

The biomimetic design principles of the drug-releasing chewing robot [48] are based on the engineering of dental occlusion principles [53–57] and physiological features [58] associated with relationships between tooth form and chewing motions [59] that define three types of food processing: shearing, crushing and grinding [23,59–62], which neither Apparatus A nor B fully take into consideration.

For optimum drug release from chewing gum, the crush/shear ratio and power stroke are used for effective chewing [60–62] to disrupt mechanical bonds through the mechanics of chewing sequences [59–62]. This considers the Frankfort-mandibular plane angle (FMA), Bennett angle (BA) of the mandible [63], and Andrews's six key principles to normal occlusion [64] and occlusal

© 2025 by the author(s). Distributed under a Creative Commons CC BY license.

Preprints.org (www.preprints.org) | NOT PEER-REVIEWED | Posted: 16 June 2025 doi:10.20944/preprints202506.1212.v1

curvatures, such as the Curve of Spee in the design process [65–69]. These are: molar relationship, crown angulation, crown inclination, no rotations, no spaces and flat occlusal planes respectively [64].

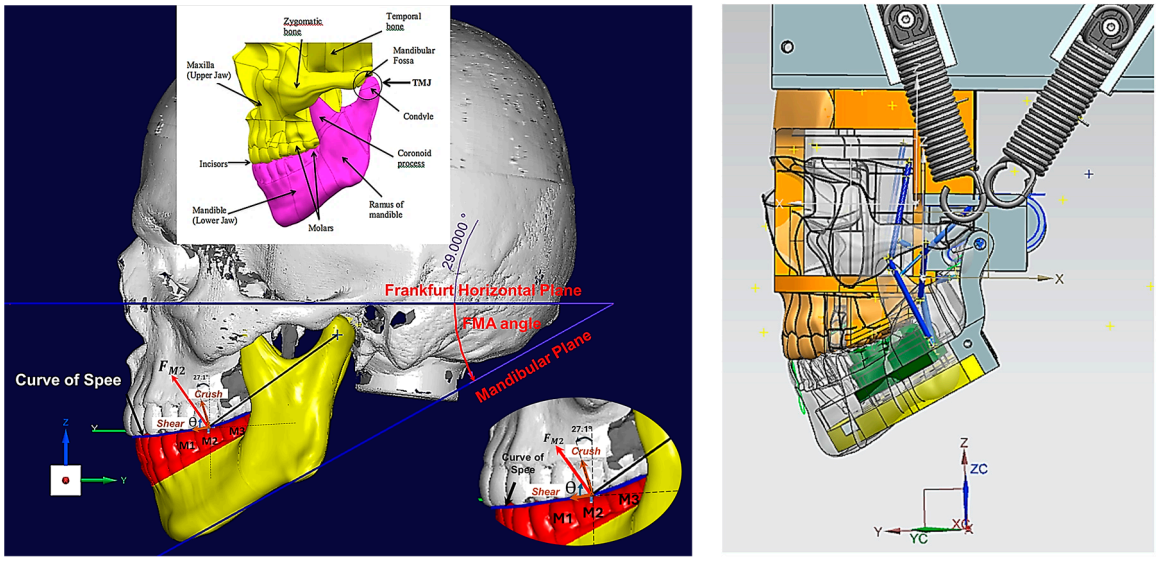

(**a**) (**b**)

Figure 1. (a) 3D CAD skeletal features of the human jaws and the FMA angle and Curve of Spee with a bite force and crush/shear represented on 2nd molar (M2); (b) 3D CAD sagittal view of humanoid chewing robot with removable chewing chamber created from biological pair.

Figures 1–6 show the design processes of the novel bio-engineered testbed which is presented in three sections: 1) bio-inspired design principles (Figures 1 and 2); 2) Instron set-ups (Figures 3 and 4); and 3) Zwick-Roell set-ups (Figures 5 and 6).

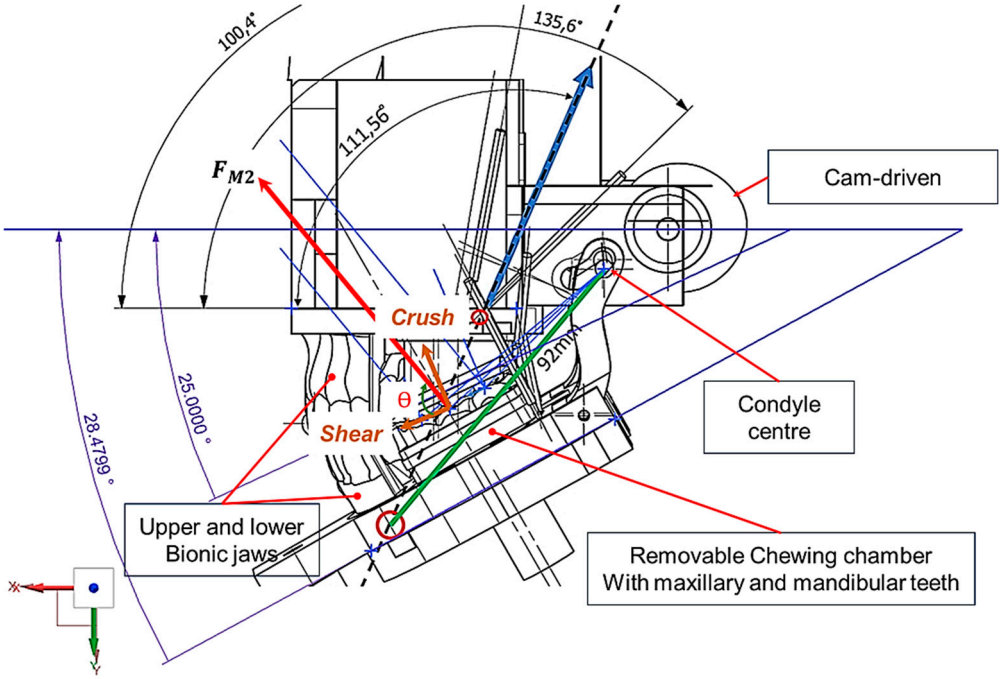

Figure 2. 3D kinematic diagram of humanoid jaws showing the removable chewing chamber with occluded mandibular and maxillary molars (M1, M2 and M3) and labels on M2.

© 2025 by the author(s). Distributed under a Creative Commons CC BY license.

Preprints.org (www.preprints.org) | NOT PEER-REVIEWED | Posted: 16 June 2025 doi:10.20944/preprints202506.1212.v1

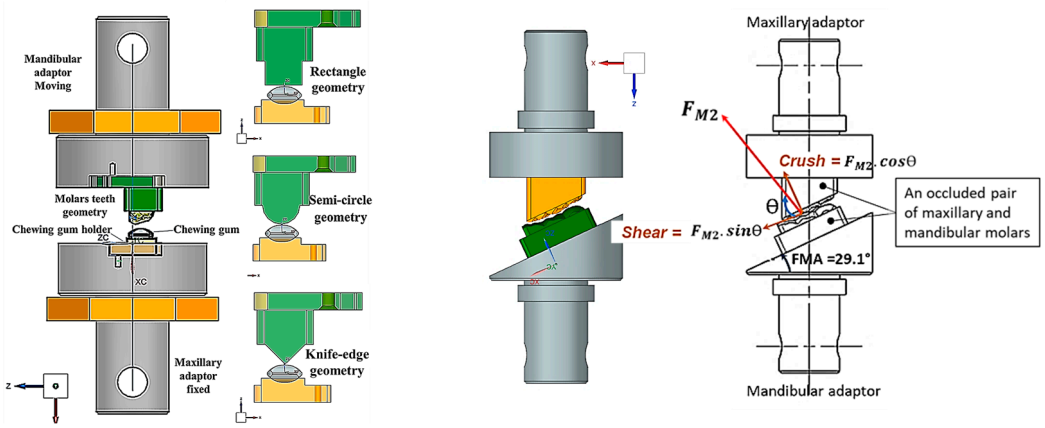

(a) (b)

Figure 3. 3D CAD bio-engineered testbed for Instron compression testing machine. (a) bio-engineered testbed with the 0° FMA for four different tooth designs integrated in the maxillary and mandibular adaptors; (b) bio-engineered testbed with the 29.1° FMA and occluded pair of mandibular and maxillary molars (M1, M2 and M3) and labels on M2.

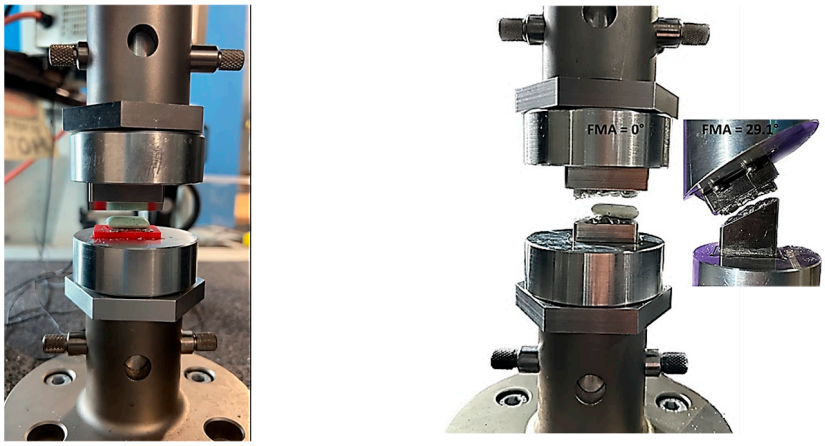

(a) (b)

Figure 4. photographs of the bio-engineered testbed setup with the 0° and 29.1° FMAs for an Instron compression testing machine. (a) shows the knife-edge geometry design; (b) shows occluded pair of mandibular and maxillary molars design.

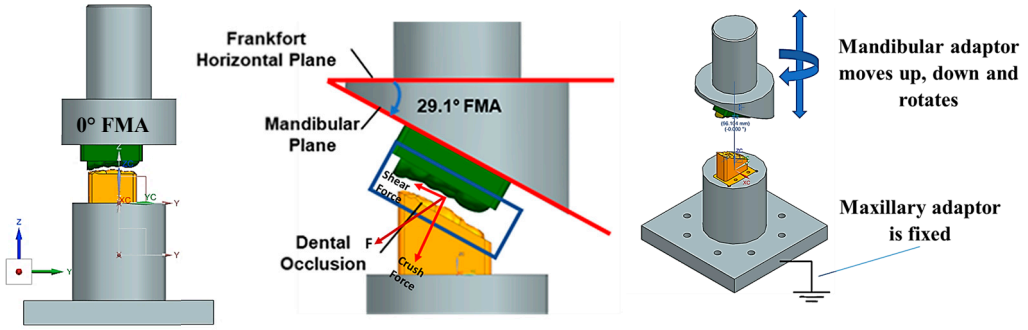

(a) (b) (c)

Figure 5. 3D CAD bio-engineered testbed for Zwick-Roell compression and torsion testing machine. (a) and (b) show bio-engineered testbed with the 0° and 29.1° FMAs and FHP and MP planes respectively; c) illustration of

© 2025 by the author(s). Distributed under a Creative Commons CC BY license.

Preprints.org (www.preprints.org) | NOT PEER-REVIEWED | Posted: 16 June 2025 doi:10.20944/preprints202506.1212.v1

the principle of the machine's motion with the 29.1° FMA, 8° BA, and occluded pair of mandibular and maxillary molars.

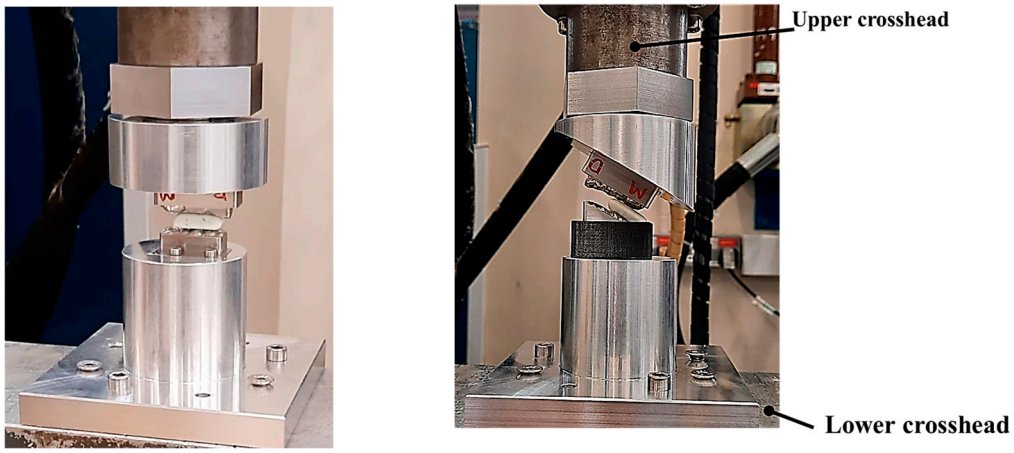

(**a**) (**b**)

Figure 6. photographs of the bio-engineered testbed setup with the 0° and 29.1° FMAs occluded pair of mandibular and maxillary molars for Zwick-Roell compression and torsion testing machine. (a) shows the 0° FMA and (b) shows 29.1° FMA.

Section 1 includes 3D CAD models of the drug-releasing chewing robot based on a SOMSO skeleton model of a human skull as a biological pair [70] (SOMSOMODELLE GmbH, Adam Rouilly, Kent, UK) which passed a scientific accuracy test [48]. The Cephalometric analysis (CeA) (Figure 1a) is also labelled with anatomical features including the Frankfurt Horizontal plane (FHP), Mandibular Plane (MP) and Curve of Spee represented the bite force or power stroke on 2nd molar. The occluded pair mandibular and maxillary molars with the integrated FMA angle in the removable chewing chamber presented in the Figure 1b. The Curve of Spee passes through the buccal cusps tips of molars to the cusp tips of the mandibular molars. Curve of Spee is regarded as the most important Andrew's 6 key principles, which is the plane of occlusion and it should be horizontal or along the Curve of Spee [64] as shown in Figure 1a. The two bilateral functional springs in Figure 1b representing the temporalis muscles. They attach to each side of the maxillary jaw to hold the mechanical mandible in the correct occlusion and balance the torque generated during chewing whilst contacting with the mandible condyles and cam-driven mechanism. Figure 2 represent further kinematic information on the design process. Within Section 2, Figure 3a shows the various designs and the associated adaptors with 0°FMA, whist Figure 3b shows CAD models with 29.1°FMA and a bite force or power stroke represented on 2nd molar. Figure 4 shows the manufactured and assembled testbed. Figures 5 and 6 provide similar representations for the Zwick-Roell set-ups in Section 3.

2.2. Two-Bite Test – Texture Profile Analysis (TPA)

TPA is a popular double-compression test for determining the textural or mechanical properties in food science [49] and pharmaceutical industry for oral drug release [28,36,37,41,50,51]. The TPA test is often called the "two-bite test" because the texture analyser intend to mimic the mouth's biting action [71].

Tests can be conducted with universal testing machines or texture analysers [49–52,72–84] where a top plate compresses a specimen to a particular compressive strain. The increasing force is measured via load cell, then the top plate returns to its original value, followed by a second compression stage to the same position as the first stage. A force-displacement or force-time response graph is generated that correlates with the mechanical properties of food [49,52,72–80,82,85–87] or MCGs [37,41,42,50,83,84,88]. The TPA parameters can be derived either directly or indirectly from response graph and be classed as primary or secondary. In Figure 7a, the initial highest peak in the

© 2025 by the author(s). Distributed under a Creative Commons CC BY license.

Preprints.org (www.preprints.org) | NOT PEER-REVIEWED | Posted: 16 June 2025 doi:10.20944/preprints202506.1212.v1

first cycle is related to the hardness of the tested materials, F_1. The appearances of minor peaks during the first cycle that precede the hardness peak are indicators of the brittleness (i.e. a material's tendency to fracture under stress with little or no plastic deformation before breaking) of the compact, F_0. The strength of the internal bonds in tested materials is defined as cohesiveness, which is calculated from the ratio of the positive areas under the graph for the first and second cycles, $\frac{A2}{A1}$. The mechanical behaviour of the tested material after the release of the applied force and the retraction of the compression probe can be related to their springiness/elasticity, which can be estimated from the time ratio between the initial points of the two cycles, $\frac{t_{B-C}}{t_{A-D}}$. Chewiness is a secondary parameter that could also be derived from the measured parameters; it is calculated as the multiplication of hardness, cohesiveness, and springiness, $F_1 \cdot \frac{A2}{A1} \cdot \frac{t_{B-C}}{t_{A-D}}$. Compressibility is the ratio between thicknesses of the tested samples before and after the two cycles of compression. It can be estimated as a percentage from the distances between A and D, d_{A-D} and between B and C, d_{B-C} respectively, $\frac{d_{A-D}+ d_{B-C}}{Original\ thickness}$. The parameters cohesiveness, springiness and chewiness relate to mastication physiology (i.e. mechanical breakdown of food). Elevated values of these textural parameters could increase chewing time, jaw movement, and muscle activity [85]. In particular, the springiness and cohesiveness provide important structural information [85], cohesiveness (i.e. the force required to sever internal bonds), chewiness (i.e. the energy required to chew a product until is ready to be swallowed) [89] and compressibility indicates how easily food can be compressed during chewing. Adhesiveness, which is a textural property more appropriate to the stickiness of foods, is defined as the force value required for a probe to overcome attractive forces (sticking) between its surface and the surface of the product being investigated [37,41,42,49,50,52,87–92]. It is represented by the negative area under the x-axis of the force-time graph at the end of the first bite as enlarged in Figure 7a. Finally, work done is determined by summing the positive areas under the force-displacement graph for each of the two highest force peaks, $A_1 + A_2$. This sum represents the energy required to deform the sample during the test [90].

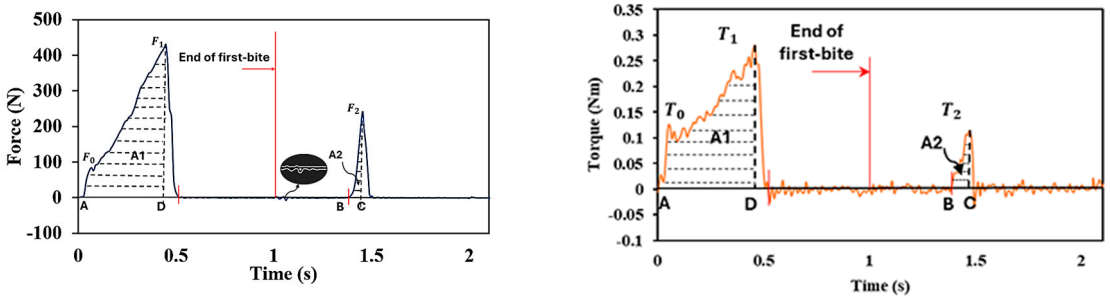

(a) (b)

Figure 7. (a) Force-time graph from a two-bite test for MCGs using occluded molars pair with 25°FMA (+/- 5° is within normal human range); (b) Torque-time graph from a two-bite test for MCGs using occluded molars pair with 25°FMA. .

In this study, the work done is more representative of human chewing in terms of bite force (or power stroke) and energy required to disrupt mechanical bonds. Bite force is primarily measured perpendicular to the Curve of Spee, and on the second molar is typically between 20-30° from the vertical (z) axis for hominids [61]. The bite force angle from the z-axis has been measured as 27.1° as shown within Figure 1a. The resultant force acting on the maxilla when the jaws occlude is often at angle to the direction of bite force and has two components: crush and shear. Pure crush forces are in-line with the bite force direction and are therefore orthogonal to the occlusal plane, which is the direction of pure shear forces. The bite force angle, θ, was measured as 71.2° which is similar to the human range that is between 55-80° [61].

Osborn [61] described the crush/shear ratio as the ratio of the orthogonal forces on the molar's occlusal plane for human chewing. In our study, we propose for the first time, to abstract accurately

© 2025 by the author(s). Distributed under a Creative Commons CC BY license.

Preprints.org (www.preprints.org) | NOT PEER-REVIEWED | Posted: 16 June 2025 doi:10.20944/preprints202506.1212.v1

the FMP plane and its geometrical relationship between occluded pair of mandibular and maxillary molars teeth as shown in Figure 1a and bio-engineered FMA angle into testbed as shown in Figure 3b and Figure 5. By measuring force and torque during the two-bite test, the crush/shear ratio can be calculated in terms of work done/energy required or power stroke as shown in Equation 1.

$$\frac{Crush}{Shear} Ratio = \frac{Work\ done\ by\ crush\ force}{Work\ done\ by\ shear\ force + work\ done\ by\ torque} \quad (1)$$

Equation 1 is used alongside of TPA parameters to prove the critical role of jaw physiology and dental morphology on the experimental results when using *in vitro* apparatus, and moreover to evaluating the novel testbed and proposing a framework for parameter optimisation.

Figure 7b shows a torque-time graph for MCGs, representing the molars shearing, crushing and grinding during a two-bite test. This sequence of three different masticatory processes is called the "power stroke of mastication", where Simpson [93] defined it into two phases. In phase I, the first movement (shearing) is on the buccal side (towards the cheek). This involves the shearing of the food by the lower molars moving upwards and lateral to a centric occlusion point, which causes the cusps of the teeth to slide past each other to tear food apart. The second movement (crushing) is on the lingual side (towards the tongue). This involves the lower teeth moving directly upwards causing the basins of the molars to enter the basins of the opposing molars which crushes the food. In phase II, the final movement (grinding), involves the mandible moving laterally with a partial azimuth rotation, resulting in the cusps and basins of the molars to slide past each other and grind food [94,95].

The chewing gum sample used in all experimental tests was Wrigley's Extra White (The Wrigley Company, Plymouth, UK) as a test sample for material uniformity with average dimensions of (22.4 x 10.8 x 6.5 mm). This was the MCG of choice for *in vitro* and *in vivo* clinical trials, containing xylitol as the investigative agent [10].

Section 1 - Bio-inspired design principles

Section 2 - Instron set-ups

Section 3 - Zwick-Roell set-ups

Figure 7 shows response graphs from a universal testing machine illustrating the general principles of two-bite test for the 25° FMA (+/- 5° is within normal human range) [96].

The experimental data is presented in Sections 3.1 to 3.5 with varying Instron and Zwick-Roell set-ups and objectives to evaluate the bio-engineered testbed. There are five Set-ups (as shown below), where Set-up A utilises the Instron machine (without torque measurement) and the others utilise the Zwick-Roell (with torque measurement). Compression rate was set at 75% of the MCG thickness for both testing machines [73]. The experiments did not incorporate any artificial saliva or temperature.

Set-up A: Instron using 10 mm/s compression and FMA = 0 to evaluate tooth morphologies (including an occluded pair of molars)

Set-up B: Zwick-Roell using 10 mm/s compression and BA = 0 whilst varying FMA

Set-up C: Zwick-Roell using 49.5 mm/s compression and BA = 0 whilst varying FMA (to emulate human chewing speed)

Set-up D: Zwick-Roell using 10 mm/s compression and BA = 8 whilst varying FMA (to evaluate the change in BA)

Set-up E: Zwick-Roell using 49.5 mm/s compression and BA = 8 whilst varying FMA (to emulate human chewing speed)

3. Results

3.1. Set-Up A: Instron Using 10 mm/s Compression and FMA = 0 to Evaluate Tooth Morphologies (Including an Occluded Pair of Molars)

Figure 8 shows the force-time response graph and its associated TPA parameter calculations (Table 1). In this instance, the work done is calculated by $(A_1 + A_2)$ rather than equation 1 because the Instron machine is not capable of measuring torque.

© 2025 by the author(s). Distributed under a Creative Commons CC BY license.

Preprints.org (www.preprints.org) | NOT PEER-REVIEWED | Posted: 16 June 2025 doi:10.20944/preprints202506.1212.v1

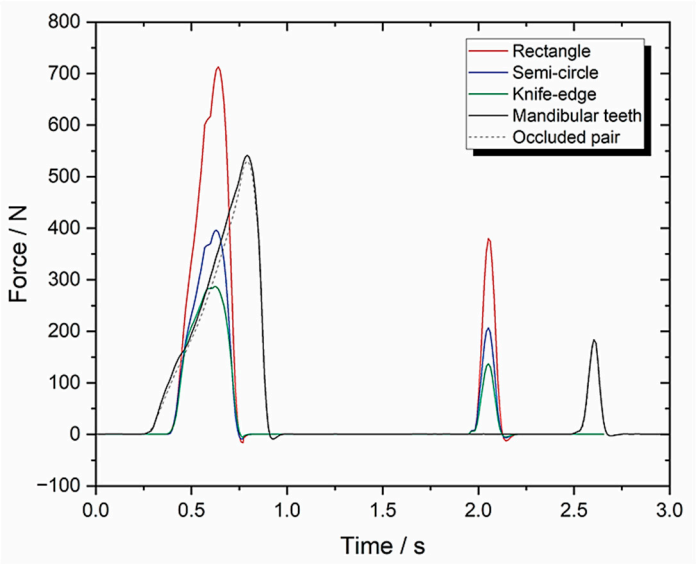

Figure 8. Shows Set-up A, (a) Force-time graph with 10 mm/s compression, 0° FMA, and 0° BA. .

Table 1. Set-up A parameters with 10 mm/s compression, 0°FMA, and 0°BA (n = 10).

TPA Parameters	Knife-edge	Rectangle or Flat	Semi-circle	Mandibular Teeth	Occluded pair of Molars Teeth
Hardness (N)	287.20	713.51	396.32	546.5	541.7
Cohesiveness	0.16	0.205	0.18	0.09	0.06
Springiness	0.29	0.33	0.28	0.242	0.225
Chewiness	13.33	48.27	19.97	11.9	7.31
Compressibility	0.44	0.52	0.44	0.75	0.827
Work Done (J)	40.74	91.07	54.17	1480.5	1448.67

3.2. Set-Up B: Zwick-Roell Using 10 mm/s Compression and BA = 0 Whilst Varying FMA

Figure 9 shows the resultant graphs and Table 2 contains the associated TPA calculations.

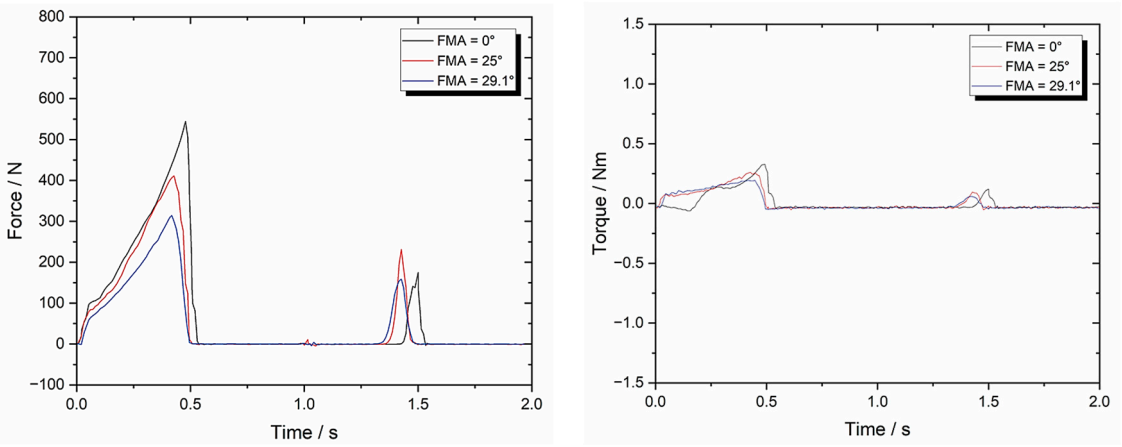

(**a**) (**b**)

Figure 9. Shows Set-up B, (a) Force-time graph with 10 mm/s compression and 0°BA; (b) Torque-time graph with 10 mm/s compression and 0°BA.

© 2025 by the author(s). Distributed under a Creative Commons CC BY license.

Preprints.org (www.preprints.org) | NOT PEER-REVIEWED | Posted: 16 June 2025 doi:10.20944/preprints202506.1212.v1

Table 2. Set-up B parameters with 10 mm/s compression and 0°BA (n = 3).

TPA Parameters	0° FMA	25° FMA	29.1° FMA
Hardness (N)	558.01	419.88	318.87
Cohesiveness	0.05	0.10	0.12
Springiness	0.10	0.17	0.20
Chewiness	2.79	7.14	7.65
Compressibility	0.82	0.87	0.89
Max Torque (Nm)	0.31	0.24	0.17
Work Done (J)	1295.05	958.67	709.18
Crush to Shear Ratio	∞	4.22	3.41

3.3. Set-Up C: Zwick-Roell Using 49.5 mm/s Compression and BA = 0 Whilst Varying FMA (to Emulate Human Chewing Speed)

Figure 10 shows the response graphs and Table 3 contains the TPA parameters.

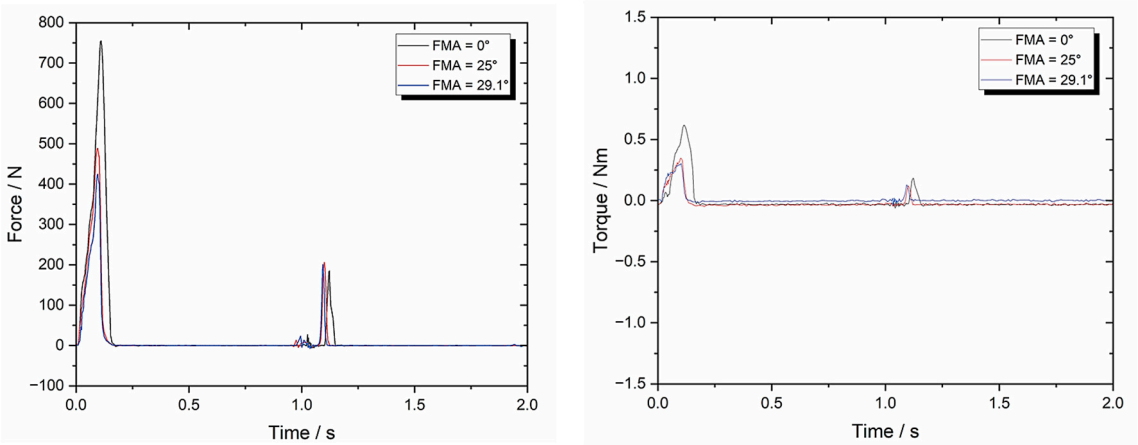

(**a**) (**b**)

Figure 10. Shows Set-up C, (a) Force-time graph with 49.5 mm/s compression and 0°BA; (b) Torque-time graph with 49.5 mm/s compression and 0°.

Table 3. Set-up C parameters with 49.5 mm/s compression and 0°BA (n = 8).

TPA Parameters	0° FMA	25° FMA	29.1° FMA
Hardness (N)	760.12	496.54	430.85
Cohesiveness	0.09	0.17	0.19
Springiness	0.29	0.21	0.22
Chewiness	19.84	17.73	18.01
Compressibility	0.92	0.83	0.86
Max Torque (Nm)	0.59	0.33	0.3
Work Done (J)	1301.71	1524.69	1421.68
Crush to Shear Ratio	∞	4.22	3.41

© 2025 by the author(s). Distributed under a Creative Commons CC BY license.

Preprints.org (www.preprints.org) | NOT PEER-REVIEWED | Posted: 16 June 2025 doi:10.20944/preprints202506.1212.v1

3.4. Set-Up D: Zwick-Roell Using 10 mm/s Compression and BA = 8 Whilst Varying FMA (to Evaluate the Change in BA)

Figure 11 shows the response graphs and Table 4 contains its TPA parameters.

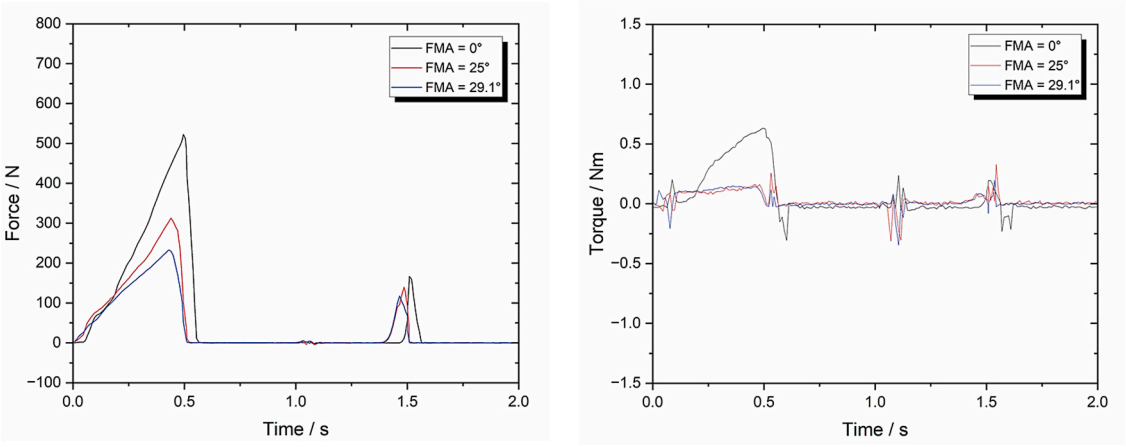

(**a**) (**b**)

Figure 11. Shows Set-up D, (a) Force-time graph with 10 mm/s compression and 8°BA; (b) Torque-time graph with 10 mm/s compression and 8°BA.

Table 4. Set-up D parameters with 10 mm/s and 8°BA (n = 8).

TPA Parameters	0° FMA	25° FMA	29.1° FMA
Hardness (N)	581.66	347.69	232.59
Cohesiveness	0.05	0.09	0.10
Springiness	0.11	0.27	0.23
Chewiness	3.2	8.45	5.35
Compressibility	0.83	0.95	0.91
Max Torque (Nm)	0.65	0.19	0.19
Work Done (J)	1292.67	805.15	590.48
Crush to Shear Ratio	26157	4.22	3.41

3.5. Set-Up E: Zwick-Roell Using 49.5 mm/s Compression and BA = 8 Whilst Varying FMA (to Emulate Human Chewing Speed)

Figure 12 shows the resultant graphs and Table 5 contains the associated TPA calculations.

Table 5. Set-up E parameters with 49.5 mm/s compression and 8°BA (n = 8).

TPA Parameters	0° FMA	25° FMA	29.1° FMA
Hardness (N)	793.47	446.75	294.36
Cohesiveness	0.06	0.11	0.13
Springiness	0.19	0.23	0.23
Chewiness	9.04	11.3	8.8
Compressibility	0.84	0.84	0.85
Max Torque (Nm)	0.96	0.45	0.38
Work Done (J)	1971.80	1123.21	791.09
Crush to Shear Ratio	19634	4.22	3.41

© 2025 by the author(s). Distributed under a Creative Commons CC BY license.

Preprints.org (www.preprints.org) | NOT PEER-REVIEWED | Posted: 16 June 2025 doi:10.20944/preprints202506.1212.v1

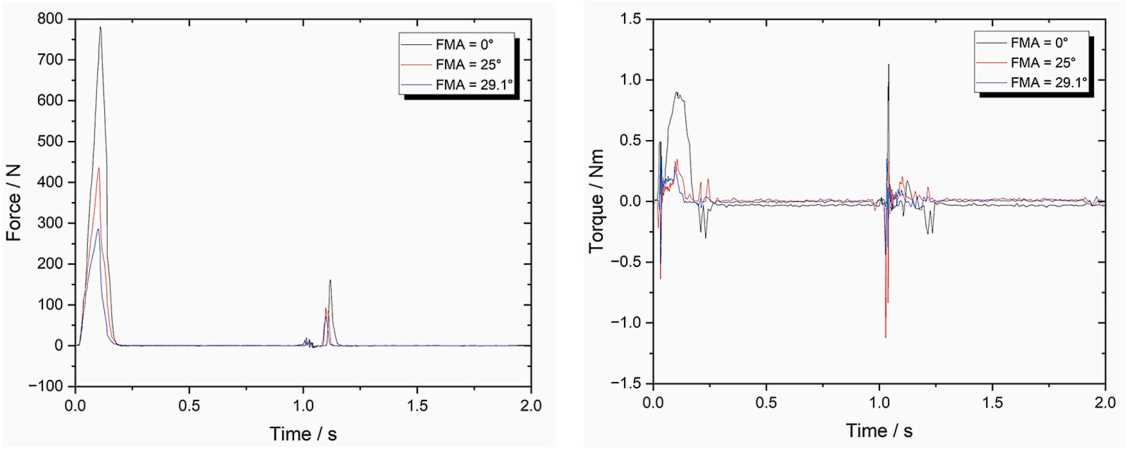

(**a**) (**b**)

Figure 12. shows Set-up E, (a) Force-time graph with 49.5 mm/s compression and 8°BA; (b) Torque-time graph with 49.5 mm/s compression and 8°BA.

4. Discussion

Beginning with **Set-up A**, Figure 8 shows the force-time response graph and its associated TPA parameter calculations (Table 1). The objective was to demonstrate that human replica teeth, particularly the occluded pair of molars were more effective for chewing in terms of morphology than other, simpler geometries as shown in Figure 3.

As a reference, Al Hagbani and co-workers [50] tested the mechanical properties of three commercial chewing gums, Wrigley®, Extra®, and Nicotine®. A TA-XT plus texture analyser was fitted with a flat-faced TA-4 cylindrical probe and using constant compression of 4.0 mm/s. They found the average values of: cohesiveness (0.48±0.08); springiness (0.28±0.04); chewiness (6.18±0.79); compressibility (0.92±0.08). Cohesiveness and chewiness are defined as primary and secondary parameters which were a measure of the force required to disrupt mechanical bonds and the energy required to chew a product until is ready to be swallowed respectively. These two TPA parameters are used alongside of springiness/elasticity (i.e. mechanical behaviour parameters) for direct comparison.

With a flat-faced morphology, Set-up A produced eight times the value of chewiness (48.27), similar springiness/elasticity (0.33) and half the compressibility (0.52) respectively when compared with the reference.

With a mandibular teeth morphology, Set-up A produced twice the value of chewiness (11.9), lower springiness/elasticity (0.242) and lower compressibility (0.75) respectively when compared with the reference. Table 1 provides clear evidence for the relationship between work done and teeth morphology when transitioning from primitive shapes to complex morphologies.

The data generated for the occluded pair of molars is closely comparable to the reference values except for the cohesiveness result (0.06) which is much higher in Al Hagbani and co-workers. This parameter is associated to the strength of the internal bonds and it demonstrates the effectiveness of power stroke from occluded pair of molars to break mechanical bonds.

For Set-up B using the Zwick-Roell device, Figure 9 shows the resultant graphs and Table 2 contains the associated TPA calculations. The two objectives were to compare the set-ups using FMA = 0, and then to evaluate how increasing the FMA angle affects biting forces with respect to the crush/shear ratio and the work done.

When using an occluded pair of molars with FMA = 0, both set-ups generate similar results, although the springiness and chewiness are slightly lower (0.225/0.10 and 7.31/2.79 respectively). However, the sample size for Set-up B was lower (3 rather than 10) which does provide a less representative average.

© 2025 by the author(s). Distributed under a Creative Commons CC BY license.

Preprints.org (www.preprints.org) | NOT PEER-REVIEWED | Posted: 16 June 2025 doi:10.20944/preprints202506.1212.v1

After increasing the FMA from 0 to 25, there is noticeable difference in some of the TPA parameters: specifically, the hardness decreases by 33 %, the chewiness increases by 256 %, and the work done is reduced by 35 %. Raising the FMA from 25 to 29.1 generates another noticeable decrease to the hardness and work done values, which results in a lower crush/shear ratio (4.22 to 3.41).

This is clear evidence of the effectiveness of altering the FMA in terms of chewing efficiency and shows the importance of FMA during mastication – this is critical for drug release and provides some validation for this bio-engineered testbed.

Figure 10 shows the response graphs for Set-up C and Table 3 contains the TPA parameters. The objective was to identify any changes to the results after increasing the compression speed to 49.5 mm/s which is comparable to the human chewing speed. The main difference was in the chewiness value, which is far higher – the remaining parameters were elevated slightly, but there was no change in the crush/shear ratio when increasing the FMA.

Figure 11 shows the response graphs and Table 4 contains the TPA parameters for Set-up D. The objective was to identify the effect of BA on the calculated mechanical properties.

In comparison to Set-up B that implemented BA = 0, the results with BA = 8 are very similar when FMA = 0. However, once the FMA rises to 25 and 29.1, clear reductions in the hardness are visible (by 21 % and 37 % respectively), which in turn reduced the overall work done (by 19 % and 20 % respectively).

This is clear evidence that demonstrates the importance of BA on chewing efficiency.

Furthermore, Set-up E (Figure 12, Table 5) demonstrated the importance of BA at chewing speeds comparable to humans. Figure 12b clearly illustrates greater torque values (when compared to Figure 10b) are imposed on the MCG during the two-bite test which, combined with lower chewiness values, generated lower work done and thus an improved chewing efficiency. This is particularly true at higher FMAs which yields more evidence of the impact of both FMA and BA on TPA parameters and further validates the novel two-bite testbed in terms of chewing efficiency and power stroke.

In all the experimental set-ups the adhesiveness value had been very low. This parameter is calculated from the negative area under the x-axis at the end of the first bite (as indicated in Fig. 2). Kaushik and co-workers [97] optimised batches of MCG-2 containing promethazine for drug release using TPA and *in vitro* study with Apparatus A. They identified that chewing gum with low adhesiveness values (0.10) is regarded as a positive evaluation [97]. Unfortunately, Al Hagbani and co-workers [50] did not use the adhesiveness parameter in their analysis.

These extensive experimental results are clear evidence illustrating the impact that the jaws physiology, dental morphology and form-function have on TPA parameters. Consequently, there are benefits towards *in vitro* masticatory apparatus as it was highlighted in Section 1, introduction. For MCGs drug release, A & B apparatus had limited jaws anatomical physiology as highlighted by Stomberg and co-workers [44] and Externbrink and co-workers [46]. As mentioned earlier in Section 1, Stomberg and co-workers attempted to improve apparatus B by developing 45º gliding steel unit with a four-cylindrical-cusped molar to imitate the occlusal plane of the natural dentition [44]. Despite the authors' valiant attempts, the improvement to apparatus B had limited anatomical accuracy, and the occlusal surface geometries and mastication was very simplified. This was already addressed by Alemzadeh and co-workers created a novel chewing robot with built-in humanoid jaws [10].

For dental science, Krueger and co-workers [14] tested the applicability of Artificial Resynthesis Technology (ART 5) to create microwear textures under controlled conditions replicating the oral environment. In their two chewing experimental studies, they used occluding pairs of third molars that were surgically extracted: one used dried beef and another used sand added to the dried beef. Their preliminary results showed that ART 5 as a dental simulator produces microwear textures and concluded that these results indicate its potential to untangle the complex variables of dental microwear formation. A more thorough experimental protocol would be necessary with ART 5 to improve controls, pH of the simulated oral environment, and grit measurements. It is interesting to

© 2025 by the author(s). Distributed under a Creative Commons CC BY license.

Preprints.org (www.preprints.org) | NOT PEER-REVIEWED | Posted: 16 June 2025 doi:10.20944/preprints202506.1212.v1

note that occluding pairs of third molars were used in their study. In this study, more pairs of molars (M1, M2 and M3) were integrated which is a more realistic representation of the human jaw and it is beneficial for food fracturing *in vitro* apparatus [6] or even two-bite test.

For food science, as highlighted in Section 1, comprehensive review of systematic designs over the past 15 years by Guo and co-workers [19] highlighted the current limitations of on physiological structures of masticatory simulators, stating there is no established methods/criteria for evaluating their biomimetic components. The manuscript clearly addresses testing methods, standardising chewing efficiency, and criteria for evaluating the biomimetic components [19] with the PLM framework with built-in reverse biomimetics methodology developed by Alemzadeh [48].

Walker and co-workers [20] investigated the effect of dental morphology, form-function and comminution chewing experiments in catarrhines using the BA chewing simulator developed by Salles et al. [6] for food fracturing. The size of molars used in the chewing simulator were all equal due to simplifying some aspects of mastication (i.e. as a trade-off), knowing that tooth size has an influence on the fragmentation of certain types of food, in terms of mechanics. They proposed other simulators under development [10,14,24,25] may allow further studies on the form-function relationships of teeth. This relationship is investigated by integrating the occluded pair of molars integrated into the bio-engineered testbed based on Ref. [10], developed by Alemzadeh.

Within Section 3, the results clearly illustrating the effectiveness of tooth morphology with respect to chewing efficiency and effective mastication for drug release from MCGs. The major advantage and benefit of the novel bio-testbed is that it can be used with universal testing machines and provides a better framework and future direction in two-bite test.

To this date, still new apparatus is constantly being developed based on biomimetics and bio-inspired design [98].

5. Conclusions

A novel bio-engineered two-bite testbed was created for two universal testing machines with compression and torsion based on bionics design principles for accurate comminution and molars intercuspation and effective mastication in terms of mechanochemistry and power stroke to break mechanical bonds.

Extensive experimental studies with different setups for FMA and BA [63] were conducted to systematically analyse a two-bite test to evaluate the mechanical properties of MCGs and to probe the form-function relationships between biting force and crushing/shearing aspects to understand chewing efficiency and effective power stroke of mastication. The manuscript critically analysed the impact and importance of jaw physiology, dental morphology, and FMA and BA angles on two-bite test parameters, validating the bio-engineered testbed for API release from MCGs. This work also has impact on other fields that use *in vitro* masticatory apparatus as critically analysed and discussed in Sections 1 and 4 respectively. This proof of concept (POC) chewing platform could be used to validate drugs such as aspirin, caffeine, CPP-ACP, dimenhydrinate, chlorhexidine contained within commercially available MCG and administered for pain relief, as a central-nervous-system (CNS) stimulant, tooth decay, motion sickness, and dental hygiene respectively.

Our innovative approach combined the fields of bionics, bioengineering, dental biomechanics, and biomedical engineering to address a significant barrier in the commercial development of MCG [10,48]. The research group's vision is to use and optimise this enabling technology to test tailored drug release from MCG to determine API doses that would be received by patients in a controlled, safe, and user-friendly manner, that would also reduce development costs. This advancement in drug delivery technology has the potential to improve patient care and outcomes as functional chewing gums for health are growing in popularity and the market is expected to reach $3.18 billion by 2028 [99].

6. Patents

© 2025 by the author(s). Distributed under a Creative Commons CC BY license.

Preprints.org (www.preprints.org) | NOT PEER-REVIEWED | Posted: 16 June 2025 doi:10.20944/preprints202506.1212.v1

Dental simulator—Kazem Alemzadeh https://patents.google.com/patent/US20090035739A1/en (accessed 31/5/2025)

Author Contributions: Conceptualization, K.A.; methodology, K.A.; formal analysis, K.A.; investigation, K.A.; resources, K.A; data curation, K.A., J.A; writing—original draft preparation, K.A., J.A.; writing—review and editing, K.A., J.A,; visualization, K.A, J.A. Both authors have read and agreed to the published version of the manuscript.

Funding: This research received no external funding.

Institutional Review Board Statement: Favourable ethical approval was granted for a drug-releasing chewing robot study by the University of Bristol Faculty of Health Sciences Research Ethics Committee. Application No. 30882 [10].

Informed Consent Statement: Not applicable.

Data Availability Statement: : Data are unavailable due to privacy.

Acknowledgments: The first author acknowledges his gratitude to technicians and expert machinists from the Queens Building Mechanical Workshop for continuous support and their assistance over the years.

Conflicts of Interest: The authors declare no conflicts of interest.

Abbreviations

The following abbreviations are used in this manuscript:

MCG	Medicated chewing gum
PLM	Product lifecycle management
API	Active pharmaceutical ingredient
BA	Bennett angle of mandible
FMA	Frankfort-mandibular plane angle
CUR	Curcumin
TPA	Texture profile analysis
CeA	Cephalometric analysis
FHP	Frankfurt Horizontal plane
MP	Mandibular Plane
ART	Artificial Resynthesis Technology
CNS	Central-Nervous-System
POC	Proof of Concept
CPP-ACP	Casein Phosphopeptide-Amorphous Calcium Phosphate
CUR	Curcumin

References

1. Alemzadeh, K. and Raabe, D., Prototyping artificial jaws for the robotic dental testing simulator. *Proc. Inst. Mech. Eng. H*. **2008**, 222(8), pp. 1209–1220.
2. Grau, A., Stawarczyk, B., Roos, M., Theelke, B. and Hampe, R., Reliability of wear measurements of CAD-CAM restorative materials after artificial aging in a mastication simulator. *J. Mech.Behav. Biomed. Mater.* **2018**, 86, pp. 185–190.
3. Steiner, M., Mitsias, M.E., Ludwig, K. and Kern, M., In vitro evaluation of a mechanical testing chewing simulator. *Dent. Mater.* **2009**, 25(4), pp. 494–499.
4. Morell, P., Hernando, I. and Fiszman, S.M., Understanding the relevance of in-mouth food processing. A review of in vitro techniques. *Trends Food Sci. Tech.* **2014**, 35(1), pp. 18–31.
5. Peyron, M.A. and Woda, A., An update about artificial mastication. *Food Sci.* **2016**, 9, pp. 21–28.
6. Salles, C., Tarrega, A., Mielle, P., Maratray, J., Gorria, P., Liaboeuf, J. and Liodenot, J.J., Development of a chewing simulator for food breakdown and the analysis of in vitro flavor compound release in a mouth environment. *J. Food Eng*. **2007**, 82(2), pp. 189–198.

© 2025 by the author(s). Distributed under a Creative Commons CC BY license.

Preprints.org (www.preprints.org) | NOT PEER-REVIEWED | Posted: 16 June 2025 doi:10.20944/preprints202506.1212.v1

7. Woda, A., Mishellany-Dutour, A., Batier, L., François, O., Meunier, J.P., Reynaud, B., Alric, M. and Peyron, M.A., Development and validation of a mastication simulator. *J. Biomechanics*, **2010**, 43(9), pp. 1667–1673.
8. Christrup, L.L. and Moeller, N., Chewing gum as a drug delivery system. *Arch. Pharm. Chem. Sci. Ed*. **1986**, 14, pp. 30–36.
9. Kvist, C., Andersson, S.B., Fors, S., Wennergren, B. and Berglund, J., Apparatus for studying in vitro drug release from medicated chewing gums. International journal of pharmaceutics, *Int. J. Pharm.* **1999**, 189(1), pp. 57–65.
10. Alemzadeh, K., Jones, S.B., Davies, M. and West, N., Development of a chewing robot with built-in humanoid jaws to simulate mastication to quantify robotic agents release from chewing gums compared to human participants. *IEEE Trans. Biomed. Eng*. **2020**, 68(2), pp492-504.
11. Vincent, J., Biomimetics with Trade-Offs. *Biomimetics*, **2023**, 8(2), p.265.
12. Swiderski, D.L. and Zelditch, M.L., Complex adaptive landscape for a "Simple" structure: The role of trade-offs in the evolutionary dynamics of mandibular shape in ground squirrels. *Evolution*, **2022**, 76(5), pp.946-965.
13. Heintze, S.D., Reichl, F.X. and Hickel, R., Wear of dental materials: Clinical significance and laboratory wear simulation methods—A review. *Dent. Mater. J.* **2019**, 38(3), p.343-353.
14. Krueger, K.L., Chwa, E., Peterson, A.S., Willman, J.C., Fok, A., van Heel, B., Heo, Y., Weston, M. and DeLong, R., Artificial Resynthesis technology for the experimental formation of dental microwear textures. *Am. J. Phys. Anthropol.* **2021**, 176(4), pp.703-712.
15. Daegling, D.J., Hua, L.C. and Ungar, P.S., The role of food stiffness in dental microwear feature formation. *Arch. Oral Biol.* **2016**, 71, pp.16-23.
16. Pu, D., Shan, Y., Wang, J., Sun, B., Xu, Y., Zhang, W. and Zhang, Y., Recent trends in aroma release and perception during food oral processing: *Crit. Rev. Food Sci. Nutr.* **2024**, 64(11), pp.3441-3457.
17. Krause, A.J., Henson, L.S. and Reineccius, G.A., Use of a chewing device to perform a mass balance on chewing gum components. *Flavour Fragr. J.* **2011**, 26 (1), pp.47–54.
18. Peyron, M.A., Santé-Lhoutellier, V., Dardevet, D., Hennequin, M., Remond, D., François, O. and Woda, A., Addressing various challenges related to food bolus and nutrition with the AM2 mastication simulator. *Food Hydrocoll*. **2019**, 97, p.105229.
19. Guo, Y., Zhao, Q., Li, T. and Mao, Q., Masticatory simulators based on oral physiology in food research: A systematic review. *J. Texture Stud.* **2024**, 55(5), p.e12864.
20. Walker, A.E., Guy, F., Salles, C., Thiery, G. and Lazzari, V., Assessment of comminution capacity related to molar intercuspation in catarrhines using a chewing simulator. *BMSAP*, **2022**, 34(34 (2)).
21. Lucas, P.W., Corlett, R.T. and Luke, D.A., Postcanine tooth size and diet in anthropoid primates. *Z. Morphol. Anthropol.* **1986**, pp. 253-276.
22. Lucas, P.W., Dental functional morphology: how teeth work. Cambridge University Press, **2004**.
23. Berthaume, M.A., Dumont, E.R., Godfrey, L.R. and Grosse, I.R., The effects of relative food item size on optimal tooth cusp sharpness during brittle food item processing. *J. R. Soc. Interface.* **2014**, 11(101), p.20140965.
24. Jeannin, C., Gritsch, K., Liodénot, J.J. and Grosgogeat, B., MARIO: the first chewing bench used for ageing and analysis the released compounds of dental materials. *CMBBE.* **2019**, 22(sup1), pp.S62-S64, 2019.
25. Chen, B., Dhupia, J.S., Morgenstern, M.P., Bronlund, J.E. and Xu, W., Development of a biomimetic masticating robot for food texture analysis. *J. Mech. Robot.* **2022**, 14(2), p.021012.
26. Rathbone, M.J., Şenel, S. and Pather, I., Design and development of systemic oral mucosal drug delivery systems. *Oral Mucosal Drug Delivery and Therapy*, **2015**, pp.149-167.
27. Wanasathop, A. and Li, S.K., Iontophoretic drug delivery in the oral cavity. *Pharm.* **2018**, 10(3), p.121.
28. Al Hagbani, T. and Nazzal, S., Medicated chewing gums (MCGs): composition, production, and mechanical testing. *AAPS PharmSciTech*, **2018**, 19(7), 2908-2920.
29. Rassing, M.R., Chewing gum as a drug delivery system. *Adv. Drug. Deliv. Rev.* **1994**, 13(1-2), pp.89-121.
30. Ferrazzano, G.F., Cantile, T., Coda, M., Alcidi, B., Sangianantoni, G., Ingenito, A., Di Stasio, M. and Volpe, M.G., In vivo release kinetics and antibacterial activity of novel polyphenols-enriched chewing gums. *Molecules*, **2016**, 21(8), p.1008.

© 2025 by the author(s). Distributed under a Creative Commons CC BY license.

Preprints.org (www.preprints.org) | NOT PEER-REVIEWED | Posted: 16 June 2025 doi:10.20944/preprints202506.1212.v1

31. Giacaman, R.A., Maturana, C.A., Molina, J., Volgenant, C. and Fernández, C.E., Effect of casein phosphopeptide-amorphous calcium phosphate added to milk, chewing gum, and candy on dental caries: a systematic review. *Caries Res.* **2023**, 57(2), pp.106–118.
32. Kassebaum, N.J., Bernabé, E., Dahiya, M., Bhandari, B., Murray, C.J.L. and Marcenes, W., Global burden of untreated caries: a systematic review and metaregression. *J. Dent. Res.* **2015**, 94(5), pp650-658.
33. GBD 2017 Oral Disorders Collaborators, Bernabe, E., Marcenes, W., Hernandez, C.R., Bailey, J., Abreu, L.G., Alipour, V., Amini, S., Arabloo, J., Arefi, Z. and Arora, A., Global, regional, and national levels and trends in burden of oral conditions from 1990 to 2017: a systematic analysis for the global burden of disease 2017 study. *J. Dent. Res.* **2020**, 99(4), pp.362–373.
34. Aspirin Market Size, Share, Value and Forecast 2030, https://www.zionmarketresearch.com (accessed 31 /5/2025)
35. Global Vitamin C Market Size & Share to Surpass $1.8 Bn by (https://www.globenewswire.com (accessed 31 /5/2025)
36. Al Hagbani, T. and Nazzal, S., Curcumin complexation with cyclodextrins by the autoclave process: Method development and characterization of complex formation. *Int. J. Pharm.* **2017**, 520(1-2), pp.173–180.
37. Al Hagbani, T., Altomare, C., Kamal, M.M. and Nazzal, S., Mechanical characterization and dissolution of chewing gum tablets (CGTs) containing co-compressed health in gum® and curcumin/cyclodextrin inclusion complex. *AAPS PharmSciTech*, **2018**, 19, pp.3742-3750.
38. Daniell, H., Nair, S.K., Esmaeili, N., Wakade, G., Shahid, N., Ganesan, P.K., Islam, M.R., Shepley-McTaggart, A., Feng, S., Gary, E.N. and Ali, A.R., Debulking SARS-CoV-2 in saliva using angiotensin converting enzyme 2 in chewing gum to decrease oral virus transmission and infection. *Mol. Ther.* **2022**, 30(5), pp.1966-1978.
39. Imfeld, T., Chewing gum—facts and fiction: a review of gum-chewing and oral health. *Crit. Rev. Oral. Biol. Med.* **1999**, 10(3), pp.405-419.
40. Konar, N., Palabiyik, I., Toker, O.S. and Sagdic, O., Chewing gum: Production, quality parameters and opportunities for delivering bioactive compounds. Trends in food science & technology. *Trends Food Sci. Technol.* **2016**, 55, pp.29-38.
41. Al Hagbani, T. and Nazzal, S., Development of postcompressional textural tests to evaluate the mechanical properties of medicated chewing gum tablets with high drug loadings. Journal of Texture Studies. *J. Text. Stud.* **2018**, 49(1), pp.30-37.
42. Maslii, Y., Kolisnyk, T., Ruban, O., Yevtifieieva, O., Gureyeva, S., Goy, A., Kasparaviciene, G., Kalveniene, Z. and Bernatoniene, J., Impact of compression force on mechanical, textural, release and chewing perception properties of compressible medicated chewing gums. *Pharm.* **2021**, 13(11), p.1808.
43. Monograph 2.9.25 (**2012**). In Ph.Eur.9.0.
44. Stomberg, C., Kanikanti, V.R., Hamann, H.J. and Kleinebudde, P., Development of a new dissolution test method for soft chewable dosage forms. *AAPS PharmSciTech.* **2018**, 18, pp.2446-2453.
45. Zieschang, L., Klein, M., Krämer, J. and Windbergs, M., In vitro performance testing of medicated chewing gums. *Dissolut. Technol.* **2018**, 25 (3), pp.64-69.
46. [46] Externbrink, A., Sharan, S., Sun, D., Jiang, W., Keire, D. and Xu, X., An in vitro approach for evaluating the oral abuse deterrence of solid oral extended-release opioids with properties intended to deter abuse via chewing. *Int. J. Pharm.* **2019**, 561:305-313.
47. Cai, F., Shen, P., Walker, G.D., Reynolds, C., Yuan, Y. and Reynolds, E.C., Remineralization of enamel subsurface lesions by chewing gum with added calcium. *J. Dent.* **2009**, 37(10), pp.763-768.
48. Alemzadeh, K., Innovative Bionics Product Life-Cycle Management Methodology Framework with Built-In Reverse Biomimetics: From Inception to Clinical Validation. *Biomimetics*, **2025**, 10(3), p.158.
49. Schreuders, F.K., Schlangen, M., Kyriakopoulou, K., Boom, R.M. and van der Goot, A.J., Texture methods for evaluating meat and meat analogue structures: A review. *Food Control*, **2021**, 127, p.108103.
50. Al Hagbani, T., Altomare, C., Salawi, A. and Nazzal, S., D-optimal mixture design: Formulation development, mechanical characterization, and optimization of curcumin chewing gums using oppanol® B 12 elastomer as a gum-base. *Int. J. Pharm.* **2018**, 553(1-2), pp.210-219.

© 2025 by the author(s). Distributed under a Creative Commons CC BY license.

Preprints.org (www.preprints.org) | NOT PEER-REVIEWED | Posted: 16 June 2025 doi:10.20944/preprints202506.1212.v1

51. Bogdan, C., Hales, D., Cornilă, A., Casian, T., Iovanov, R., Tomuță, I. and Iurian, S., Texture analysis–A versatile tool for pharmaceutical evaluation of solid oral dosage forms. *Int. J. Pharm.* **2023**, 638, p.122916.
52. Peleg, M., The instrumental texture profile analysis revisited. *J. Texture Stud.* **2019**, 50(5), pp.362-368.
53. Benazzi, S., Grosse, I.R., Gruppioni, G., Weber, G.W. and Kullmer, O., Comparison of occlusal loading conditions in a lower second premolar using three-dimensional finite element analysis. *Clin. Oral. Investig.* **2014**, 18, pp. 369–375.
54. Katona, T.R. and Eckert, G.J., The mechanics of dental occlusion and disclusion. *Clin. Biomechanics*, **2017**, 50, pp. 84–91.
55. Katona, T.R., An engineering analysis of dental occlusion principles. *Amer. J. Orthodontics Dentofacial Orthoped.* **2009**, 135(6), pp.696-e1.
56. Katona, T.R., Engineering analyses of the link between occlusion and temporomandibular joint disorders. *J. Stomat. Occ. Med.* **2013**, 6, pp. 16–21.
57. Katona, T.R., Isikbay, S.C. and Chen, J., An analytical approach to 3D orthodontic load systems. *Angle Orthod.* **2014**, 84(5), pp. 830–838.
58. Bourdiol, P. and Mioche, L., Correlations between functional and occlusal tooth-surface areas and food texture during natural chewing sequences in humans. Archives Oral Biol., 2000, 45(8), pp.691-699.
59. Ungar, P.S., Mammalian dental function and wear: a review. *Biosurf. Biotribol.* **2015**, 1(1), pp. 25–41.
60. Osborn, J.W., Relationship between the mandibular condyle and the occlusal plane during hominid evolution: some of its effects on jaw mechanics. *Amer. J. Phy. Anthropol.* **1987**, 73(2), pp.193-207.
61. Osborn, J.W., Orientation of the masseter muscle and the curve of Spee in relation to crushing forces on the molar teeth of primates. *Amer. J.Phys. Anthropol.* **1993**, 92(1), pp.99-106.
62. Fukoe, H., Basili, C., Slavicek, R., Sato, S. and Akimoto, S., Three-dimensional analyses of the mandible and the occlusal architecture of mandibular dentition. *J. Stomat. Occ. Med.* **2012**, 5, pp. 119–129.
63. Cimić, S., Simunković, S.K. and Catić, A., The relationship between Angle type of occlusion and recorded Bennett angle values. *J. Prosthet. Dent.* **2016**, 115(6), 729–735.
64. Andrews, L.F., The six keys to normal occlusion. *Amer. J. Orthod.* **1972**, 62(3), pp.296-309.
65. Nam, S.E., Park, Y.S., Lee, W., Ahn, S.J. and Lee, S.P., Making three-dimensional Monson's sphere using virtual dental models. *J. Dent.* **2013**, 41(4), pp.336-344.
66. Spee, F.G., Biedenbach, M.A., Hotz, M. and Hitchcock, H.P., The gliding path of the mandible along the skull. *J. Amer.Dent. Assoc.* **1980**, 100(5), pp.670-675.
67. Marshall, S.D., Caspersen, M., Hardinger, R.R., Franciscus, R.G., Aquilino, S.A. and Southard, T.E., Development of the curve of Spee. *Amer. J. Orthod. Dentofacial. Orthop.* **2008**, 134(3), pp.344-352.
68. Lynch, C.D. and McConnell, R.J., 2002. Prosthodontic management of the curve of Spee: use of the Broadrick flag. *J. Prosthet. Dent.* **2002**, 87(6), pp.593-597.
69. Monson, G.S., 1932. Applied mechanics to the theory of mandibular movements. *Dent. Cosmos.* **1982**, 74, pp. 1039–1053.
70. Artificial Human Skull (Separates into 3 Parts). Available online: https://www.adam-rouilly.co.uk/product/po10-artificial-human-skull-separates-into-3-parts (accessed 31/5/2025).
71. https://texturetechnologies.com/resources/texture-profile-analysis (accessed 31/5/2025)
72. BOURNE, M.C., Texture measurement of individual cooked dry beans by the puncture test. *J. Food Sci.* **1972**, 37(5), pp.751-753.
73. Rosenthal, A.J., Texture profile analysis–how important are the parameters?. Journal of texture studies, *J. Text. Stud.* **2010**, 41(5), pp.672-684.
74. Madieta, E., Symoneaux, R. and Mehinagic, E., Textural properties of fruit affected by experimental conditions in TPA tests: an RSM approach. *IJFST*, **2011**, 46(5), pp.1044-1052.
75. Rahman, M.S., Al-Attabi, Z.H., Al-Habsi, N. and Al-Khusaibi, M., Measurement of instrumental texture profile analysis (TPA) of foods. *Techniques to Measure Food Safety and Quality: Microbial, Chemical, and Sensory*, **2021**, pp.427-465.
76. Nishinari, K. and Fang, Y., Perception and measurement of food texture: Solid foods. *J. Texture Stud.* **2018**, 49(2), pp.160-201.

© 2025 by the author(s). Distributed under a Creative Commons CC BY license.

Preprints.org (www.preprints.org) | NOT PEER-REVIEWED | Posted: 16 June 2025 doi:10.20944/preprints202506.1212.v1

77. Paredes, J., Cortizo-Lacalle, D., Imaz, A.M., Aldazabal, J. and Vila, M., Application of texture analysis methods for the characterization of cultured meat. *Sci. Rep.* **2022**, 12(1), p.3898.
78. Salejda, A.M., Janiewicz, U., Korzeniowska, M., Kolniak-Ostek, J. and Krasnowska, G., Effect of walnut green husk addition on some quality properties of cooked sausages. *LWT-FOOD SCI. TECHNOL.* **2016**, 65, pp.751-757.
79. Florek, M., Junkuszew, A., Bojar, W., Skałecki, P., Greguła-Kania, M., Litwińczuk, A. and Gruszecki, T.M., Effect of vacuum ageing on instrumental and sensory textural properties of meat from Uhruska lambs. *Ann. Anim. Sci.* **2016**, 16(2), pp.601-609.
80. Rapisarda, M., Valenti, G., Carbone, D.C., Rizzarelli, P., Recca, G., La Carta, S., Paradisi, R. and Fincchiaro, S., Strength, fracture and compression properties of gelatins by a new 3D printed tool. *J. Food Eng.* **2018**, 220, pp.38-48.
81. I. Nitschke et al., "Validation of a New Measuring Instrument for the Assessment of Bite Force". *Diagnostics*, **2023**, 13(23), p.3498.
82. Saberi, F., Azmoon, E. and Nouri, M., Effect of thermal processing and mixing time on textural and sensory properties of stick chewing gum. *Food Structure*, **2019**, 22, p.100129, 2019.
83. Mehta, F.F. and Trivedi, P., Formulation and characterization of biodegradable medicated chewing gum delivery system for motion sickness using corn zein as gum former. *Trop. j. pharm. res.* **2015**, 4(5), pp.753-760.
84. Palabiyik, I., Güleri, T., Gunes, R., Öner, B., Toker, O.S. and Konar, N., A fundamental optimization study on chewing gum textural and sensorial properties: The effect of ingredients. *Food Structure*, **2020**, 26, p.100155.
85. Jonkers, N., van Dommelen, J.A.W. and Geers, M.G.D., Intrinsic mechanical properties of food in relation to texture parameters. *Mech. Time-Depend Mater.* **2022**, 26, 323–346.
86. Nishinari, K., Fang, Y. and Rosenthal, A., Human oral processing and texture profile analysis parameters: Bridging the gap between the sensory evaluation and the instrumental measurements. *J. Texture Stud.* **2019**, 50(5), pp.369-380.
87. Foster, K.D., Woda, A. and Peyron, M.A., Effect of texture of plastic and elastic model foods on the parameters of mastication. *J. Neurophysiol.* **2006**, 95(6), pp.3469-3479.
88. Adeleke, O.A. and Abedin, S., Characterization of Prototype Gummy Formulations Provides Insight into Setting Quality Standards. *AAPS PharmSciTech.* **2024**, 25(6), p.155.
89. Lira-Morales, D., Montoya-Rojo, M.B., Varela-Bojórquez, N., González-Ayón, M., Vélez-De La Rocha, R., Verdugo-Perales, M. and Sañudo-Barajas, J.A., Dietary fiber and lycopene from tomato processing. In Plant Food by-Products: Industrial Relevance for Food Additives and Nutraceuticals (pp. 256-281). Apple Academic Press. **2018**.
90. Johnson, M., 2014. Overview of texture profile analysis, Modified October 2023, https://www.texturetechnologies.com/resources/texture-profile-analysis (accessed 31/5/2025)
91. Noren, N.E., Scanlon, M.G. and Arntfield, S.D., Differentiating between tackiness and stickiness and their induction in foods. *Trends Food Sci Technol.* **2019**, 88, pp.290-301.
92. Salahi, M.R., Mohebbi, M. and Razavi, S.M.A., Analyzing the effects of aroma and texture interactions on oral processing behavior and dynamic sensory perception: A case study on cold-set emulsion-filled gels containing limonene and menthol, *Food Hydrocoll.* **2024**, 154, p.110128.
93. Simpson, G.G., Paleobiology of Jurassic mammals. *Paleobiologica*, **1933**, 5, pp.127–158.
94. Fiorenza, L., Nguyen, H.N. and Benazzi, S., Stress Distribution and Molar Macrowear in Pongo pygmaeus: A New Approach through Finite Element and Occlusal Fingerprint Analyses. *Hum. Evol.* **2015**, 30(3-4), pp.215–226.
95. Kay, R.F. and Hiiemae, K.M., 1974. Jaw movement and tooth use in recent and fossil primates. *Am. J. Phys. Anthropol.* **1974**, 40(2):227–256.
96. DiPietro, G.J. and Moergeli Jr, J.R., Significance of the Frankfort-mandibular plane angle to prosthodontics. *J. Prosthet. Dent.* **1976**, 36(6), pp.624-635.

© 2025 by the author(s). Distributed under a Creative Commons CC BY license.

Preprints.org (www.preprints.org) | NOT PEER-REVIEWED | Posted: 16 June 2025 doi:10.20944/preprints202506.1212.v1

97. Kaushik, P., Mittal, V. and Kaushik, D., Unleashing the Potential of β–cyclodextrin Inclusion Complexes in Bitter Taste Abatement: Development, Optimization and Evaluation of Taste Masked Anti-emetic Chewing Gum of Promethazine Hydrochloride. *AAPS PharmSciTech.* **2024**, 25(6), p.169.
98. Xu, Y., Lv, B., Wu, P. and Chen, X.D., Creating similar food boluses as that in vivo using a novel in vitro bio-inspired oral mastication simulator (iBOMS-Ⅲ): The cases with cooked rice and roasted peanuts. *Food Res. Int.* **2024**, 190, p.114630.
99. Market Segmentation by Product, News, Technavio https://www.prnewswire.com, Functional Chewing Gum Market size to increase by USD 3.15 Billion between 2023 to 2028 (accessed 31/5/2025)

Disclaimer/Publisher's Note: The statements, opinions and data contained in all publications are solely those of the individual author(s) and contributor(s) and not of MDPI and/or the editor(s). MDPI and/or the editor(s) disclaim responsibility for any injury to people or property resulting from any ideas, methods, instructions or products referred to in the content.

© 2025 by the author(s). Distributed under a Creative Commons CC BY license.